Multiple Slips and Chemical Reaction Effects on unsteady MHD Heat and Mass Transfer Flow over a Permeable Stretching Sheet with Radiation

R.MohanaRamana[a]K.VenkateswaraRaju[b]J.GirishKumar[c]

[a]Department of Basic science &Humanities (Mathematics), Narasaraopeta Engineering college (Autonomous), Narasaraopeta-522601, India,mohanaramanacrypto@gmail.com

[b]Department of Freshmen Engineering (Mathematics), ChadalawadaRamanamma Engineering College (Autonomous), Tirupati-517506. India, venky.sakku@gmail.com

[c]Dept. of Mathematics, S.V.A.Government Degree College, Srikalahasthi-517634, India,drjgireeshkumar@gmaill.com

Abstract: This paper presents the results of several slips and chemical reactions on MHD unstable heat and mass transmission flow over permeable stretching layer that moves with non-uniform velocity, suction/injection, Soret effect, thermal radiation, taking into account the time-dependent magnetic field applied. The controlling partial differential equations are translated into a system of coupled nonlinear differential equations with the assistance of appropriate transformations of similarity. With the help of bvp4c with the shooting process, the corresponding equations are numerically solved. Different parameter effects on velocity, temperature, and concentration profiles are addressed with the help of graphs. The rates of skin coefficient of friction, heat and mass transfer are often concerned with the aid of tables. The study already conducted is contrasted and considered to be in substantial alignment with this analysis.

Keywords: Magneto hydrodynamics, Thermal Radiation, Soret number, Chemical reaction, Multiple slips, Stretching sheet

1. Introduction

On a no-slip state, the core principle of the theory of Navier-Stokes is established. Numerically and analytically, numerous authors have obtained solutions by taking no-slip boundary conditions to analyze the profile of velocity, temperature, and concentration outline. The flow of the boundary layer corresponding to the stretching surface was analyzed by Ali et al. (1994). In porous media, the impact of chemical reaction on free convective heat and mass transfer flow along the stretching surface was studied by Chakma et al.(2010). SwathyMukhopadhyay(2012) examined the variant of heat transmission on the boundary layer flow over a porous exponential stretching sheet by considering the existence of magnetic field velocity slip and thermal slip. The thermal radiation heat transfer and slip effects on unstable MHD flow over the stretching surface were studied by Anjali Devi et al.(2014) The partial slip and heat generation/absorption effects on hydrodynamic boundary layer flow in a porous medium over stretching surface were investigated by Abdul Hakeem et al.(2014) considering thermal radiation and wall mass transition. The hydrodynamic and thermal slip effects on MHD boundary layer flow past a nonlinear vertical stretching porous sheet have been examined by BadrAlkahtani et al. (2015). The melting heat transfer of MHD nanofluid flow over the stretching surface was researched by Mabood and Das(2016) with thermal radiation and second-order slip. Shalini Jain et al.(2018) have investigated the effect of several slips on MHD Casson fluid movement along the permeable inclined stretching melting surface by considering nonlinear radiation, non-uniform heat source, and nonlinear chemical reaction. Through considering the time-dependent magnetic field applied, Mboodet al.(2019) examined the separate slip and Soret effects on unstable heat and mass transmissin MHD flow along stretching sheet movements with non-uniform suction/injection velocity and thermal radiation. By analyzing the MHD outcomes near the stagnation point, Jawad Raja(2019) investigated the hydrodynamic slip and thermal radiation effects over a convective heated stretching sheet. Benoset al.(2019) investigated the influence of flow unsteadiness, wall slip, heat source/sink, and thermal radiation on turbulent flow along the horizontal stretching surface with thin Newtonian fluid film heat transfer. The influence of thermodiffusion in the presence of a chemical conversion on unstable Casson fluid axisymmetric flow over a time-based radially stretching layer with many slips was observed by Faraz et al.(2019). The Newtonian liquid flow porous stretching layer was investigated by Mahabaleswaret al.(2020) using the slip parameter, Darcy and Brinkman number model from Brinkman. Fenugaet al.(2020) have examined the MHD mixed convection flow and the speed of heat transfer near a stagnation point over a nonlinear vertical stretching sheet. Susheela Chowdary et al.(2020)possessed the findings of radiation, heat source/sink impact on unstable viscous incompressible laminar electrically conducting flow over the stretching surface by considering viscous dissipation.

The entire current research shows the effects of multiple slips and chemical reactions on heat and mass transmission MHD unstable flow via a permeable stretching layer that flows with non-uniform velocity, suction/injection, induction heatVia a time-dependent magnetization.

2.**Governing Equations**

We observed a two-dimensional electrically conducting MHD incompressible fluid circulation above a pores stretching wall in the presence of induction heat. The coordinate system is chosen to take the y-axis around the x-axis sheet and to take it normally, as seen in Figure.1.

By considering a $\lambda > 0$ positive constant and the sheet travels along the x-axis with non-uniform velocity $U(x,t) = \frac{ax}{(1-\lambda t)}$, the property $\lambda t < 1$stretching intensity. It is considered that the longitudinal magnetic object is the feature defined as $B(x) = B_0 x^{-1/2}$ where $B_0 \neq 0$ where the magnetic field's power is and X is the distance along the surface from the centre. As contrasted with the applied magnetic field, neglecting the generated magnetic field. Let the temperature of the free stream T_∞ be, and the concentration of the free mass be C_∞.

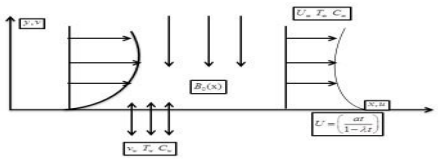

Fig.1. The physical map

The equations generated by the equations control consistency, momentum, capacity, and concentration. $\frac{\partial u}{\partial x} + \frac{\partial v}{\partial y} = 0$ (1)

$$\frac{\partial u}{\partial t} + u\frac{\partial u}{\partial x} + v\frac{\partial u}{\partial y} = \upsilon\frac{\partial^2 u}{\partial y^2} - \frac{\sigma B^2(x)u}{\rho} + g\beta_T(T - T_\infty) + g\beta_C\left(C - C_\infty\right) \quad (2)$$

$$\frac{\partial T}{\partial t} + u\frac{\partial T}{\partial x} + v\frac{\partial T}{\partial y} = \alpha\left(1 + \frac{16T_\infty^3\sigma^*}{3k^*k}\right)\frac{\partial^2 T}{\partial y^2} \quad (3)$$

$$\frac{\partial C}{\partial t} + u\frac{\partial C}{\partial x} + v\frac{\partial C}{\partial y} = D_M\frac{\partial^2 C}{\partial y^2} + D_T\frac{\partial^2 T}{\partial y^2} - Kr^*\left(C - C_\infty\right) \quad (4)$$

Where x and y are the coordinates around the substrate and natural to the sheet; u and v are the velocity components in the directions of x and y, respectively; $\rho$is the fluid density; ϑ is the fluid's kinematic viscosity; σ is the Conductivity of electricity; g is the gravity acceleration; β_T is the coefficient of thermal expansion;$\beta_c$is the coefficient of concentration; α is the coefficient of thermal diffusion; $\sigma^*$is the Stefan-Boltzmann variable $Kr^*$is the variable of the chemical reaction and K^* is the average amount of absorption.

The model's boundary conditions are defined by

$$\begin{cases} y=0: u=\mathrm{U}(x,t)+\mathrm{U}_{slip}, v=v_w, T=T_w(x,t)+\mathrm{T}_{slip}, C=C_w(x,t)+C_{slip} \\ y\to\infty: \quad u\to 0, \quad T\to T_\infty, \quad C\to C_\infty \end{cases} \tag{5}$$

$v_w=\frac{v_0}{\sqrt{x}}$ is the suction velocity $T_w(x,t)$ denotes sheet temperature and $C_w(x,t)$ indicates the surface concentration, respectively, assumed to be below.

$$T_w(x,t)=\mathrm{T}_\infty+T_0\left(\frac{ax}{2\upsilon}\right)(1-\lambda t)^{-2}, \mathrm{C}_w(x,t)=C_\infty+C_0\left(\frac{ax}{2\upsilon}\right)(1-\lambda t)^{-2} \tag{6}$$

where T_0 and C_0 temperature and concentration of the reference are such that and $0\le T_0\le T_w$ and $0\le C_0\le C_w$ the expressions above are authentic if they are valid if $(1-\lambda t)>0.$

ψ Denotes the function of the stream described as $u=\frac{\partial\psi}{\partial y}$ and $v=-\frac{\partial\psi}{\partial x}$ which meets the equation (1). The specified f,θ,ϕ and η are the following are vector dimensionless features and comparisons.

$$\begin{cases} \eta=\sqrt{\frac{a}{\upsilon(1-\lambda t)}}y \\ \psi=\sqrt{\frac{a\upsilon}{(1-\lambda t)}}xf(\eta), \\ T=T_\infty+T_0\left(\frac{ax(1-\lambda t)^{-2}}{2\upsilon}\right)\theta(\eta), \\ C=C_\infty+C_0\left(\frac{ax(1-\lambda t)^{-2}}{2\upsilon}\right)\phi(\eta) \end{cases} \tag{7}$$

Now, by substituting equations (7) into identifications (2)-(4), we have the encompasses of nonlinear odes:

$$f'''+ff''-\delta\left(\frac{\eta}{2}f''+f'\right)-Mf'+\lambda_1\theta+\lambda_2\phi=0 \tag{8}$$

$$\frac{1}{\mathrm{Pr}}(1+R)\theta''+f\theta'-f'\theta-\delta\left(\frac{\eta}{2}\theta'+2\theta\right)=0 \tag{9}$$

$$\frac{1}{\mathrm{Pr}}(1+R)\theta''+f\theta'-f'\theta-\delta\left(\frac{\eta}{2}\theta'+2\theta\right)=0 \tag{10}$$

The variant frontier circumstances of the issue are

$$f(0)=f_w, f'(0)=i+S_f f''(0), f''(\infty)=0,$$

$$\theta(0)=1+S_\theta\theta'(0),\theta(\infty)=0,\phi(0)=1+S_\phi\phi'(0),\phi(\infty)=0 \quad (11)$$

where parameters of unsteadiness, buoyancy parameters, Prandtl number, a parameter of thermal radiation, a specification of the magnetic object, Schmidt , Soret , a suction/injection specification, specification of chemical reaction represented By, $\delta=\frac{\lambda}{a}$, $\lambda_1=\frac{g\beta_T T_0}{a\upsilon}$ and $\lambda_2=\frac{g\beta_C C_0}{a\upsilon}$, $\Pr=\frac{\upsilon}{\alpha}$, $R=\frac{16T_\infty^3\sigma^*}{3k^*k}$, $Sc=\frac{\upsilon}{D_M}$, $S_r=\frac{D_T T_0}{\upsilon C_0}$ $f_w=-v_w\left(\sqrt{1-\gamma t}/\sqrt{\upsilon a}\right)$, $Kr=\frac{Kr^*}{a}(1-\lambda t)$ respectively. Impermeable surface $f_w=0$ enclosure. While the suction reflects the porous surface $f_w>0$, the fluid infusion represents the suction $f_w<0$. The local coefficient of skin friction C_f, *Nu* the local specification of Nusselt, and the local specification of Sherwood are defined as'Sh'.

$$C_f=\frac{\mu}{\rho U_w^2}\left(\frac{\partial u}{\partial y}\right)_{y=0} \quad (12)$$

$$Nu=\frac{x}{\kappa(T_w-T_\infty)}\left[\kappa\left(\frac{\partial T}{\partial y}\right)_{y=0}-\frac{4\sigma^*}{3k^*}\left(\frac{\partial T^4}{\partial y}\right)_{y=0}\right] \quad (13)$$

$$Sh=-\frac{x}{(C_w-C_\infty)}\left(\frac{\partial C}{\partial y}\right)_{y=0} \quad (14)$$

To obtain the final dimensionless form, Equations (12) are replaced by equation (7)- (14)

$$Cfr=\sqrt{\mathrm{Re}_x}C_f=f''(0),\ Nur=\frac{Nu}{\sqrt{\mathrm{Re}_x}}=-(1+R)\theta'(0),Shr=\frac{Sh}{\sqrt{\mathrm{Re}_x}}=-\phi'(0) \quad (15)$$

Where $\mathrm{Re}_x=\frac{U_w x}{\upsilon}$ the local number of Reynolds is, *Nur* is diminishes specification of Nusselt, and *Shr* is diminishes specification of shear wood *Cfr* is the reduced volume of skin friction.

3.Results and Discussions

The variant of growing the magnetic field variable 'M' on the velocity outlines without and with hydrodynamic slip as seen in Figure 2(a) and Figure 2(b), respectively. In both instances, reductions in velocity were found with a rise in magnetic specification values. The existence in the atmosphere of the transverse magnetic object movement of fluid is due to the development of the Lorentz influence, a drug-like force, which decreases the fluid's motion. However, there is an improvement in the velocity boundary layer in the presence of the hydrodynamic slip that is seen in outlines 2(a) and 2. (b). It is indicate that the boundary layer of velocity is diminished by suction. Because of this design, the suction can be used to disrupt the change from the flow of the laminar boundary layer to the stabilizing process known as turbulent boundary layer flow.

Figure 3(a), 3(b) indicates that as the magnetic variable 'M' and induction heat parameter 'R' rise, the temperature profiles enhancing. The introduction of the magnetic object physically contributes to the creation of heat in the fluid, which, in essence, decreases the amount of heat transmission from the wall, which allows the fluid temperature to rise.

The result of growing the chemical conversion specification 'Kr' and the suction parameter 'fw' on concentration profiles without and with hydrodynamic slip, respectively, as seen in Figure 4(a) and Figure 4(b). In both instances, the concentration profiles have been found to decrease with the rising simulation results of the chemical reaction. This is attributed to the assumption that the amount of solvent molecules undergoing chemical reaction is raised as the specification of chemically reaction rises, which contributes to a diminishes in the concentration region. Figures 4(a) and 4(b) also demonstrate that suction decreases the boundary layer of the concentration, contributing to a diminishes in the fluid concentration.

The impact of enhance the chemically reacted factor 'Kr' on the concentration profiles without and with thermal slip, respectively, is expressed in plots 5(a) and 5(b). In both instances, concentration profiles have been shown to be simplified with increasing parameter values of the chemical change. This suggests that as the chemical reaction rises, the solute boundary layer decreases, resulting in a drop in concentration. We also notice in Figure 5(a) and 5(b) that the concentration of the flow is diminished by suction.

The impact of increased chemical reaction specification ‘Kr’ on concentration profiles without and with solutal slip is seen in outlines 6(a) and 6(b), respectively. In both instances, the concentration profiles have been found to decrease with the rising parameter numerous of the chemically changes. Physically, as the chemical reaction rises, the solutal boundary layer reduces, which results in a concentration drop. In Figure 6(a) and 6(b), we also note that suction decreases the concentration of the flow.

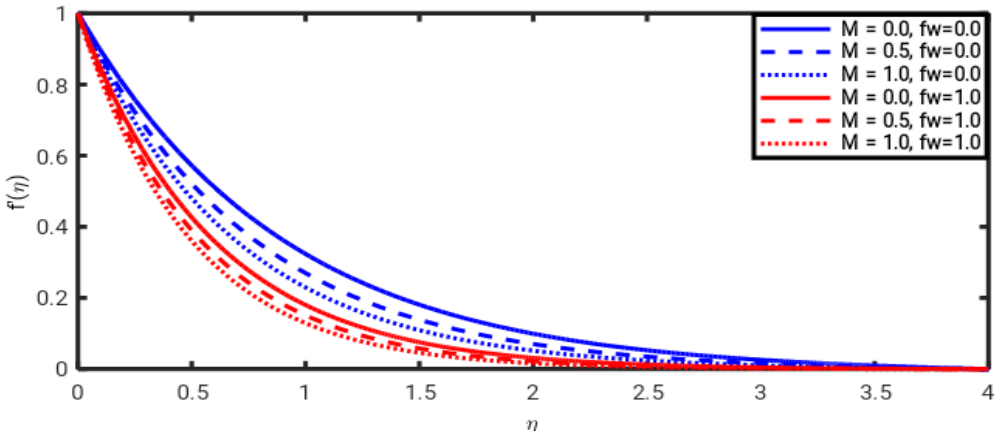

Fig.2 (a) The Variant of M and f_w on velocity with no hydro-dynamic slip when $\Pr = 1, Sc = 10, \lambda_1 = \lambda_2 = 0.2, S_f = 0, S_\theta = S_\varphi = S_r = Kr = R = \eta = \delta = 0.5$

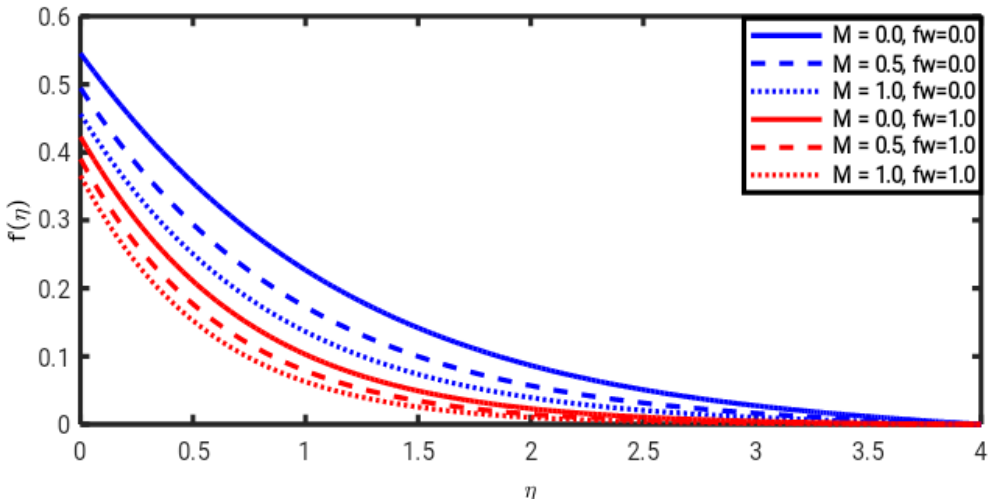

Fig.2(b) The Variant of M and f_w on velocity with hydro-dynamic slip $\Pr = 1, Sc = 10, \lambda_1 = \lambda_2 = 0.2, S_f = 1, S_\theta = S_\varphi = S_r = Kr = R = \eta = \delta = 0.5$

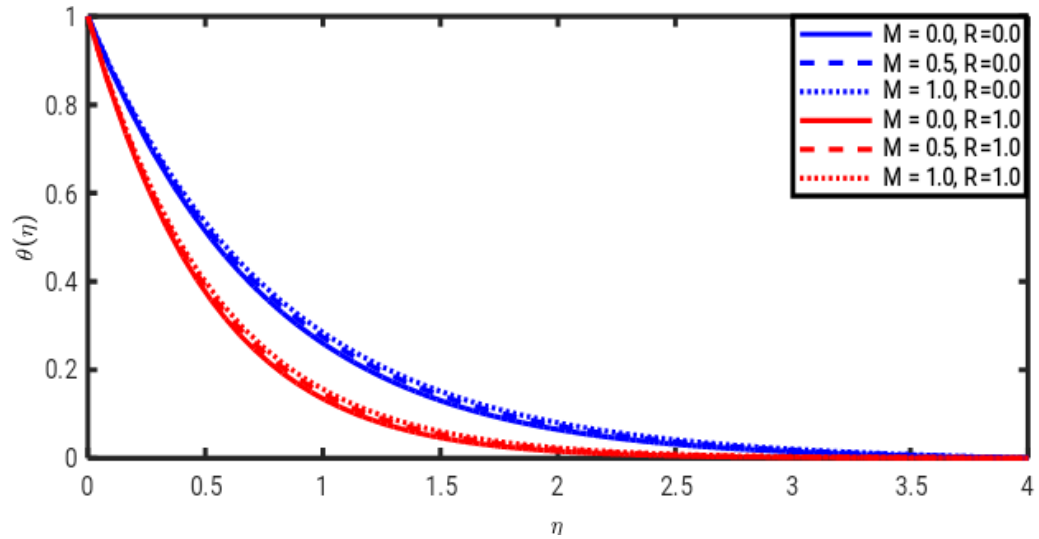

Fig.3(a) Impact of M and R with no thermal slip on temperature $\Pr = 1, Sc = 10, f_w = 0.1, \lambda_1 = \lambda_2 = 0.2, S_f = 0.5, S_\theta = 0, S_\varphi = S_r = Kr = \eta = \delta = 0.5$

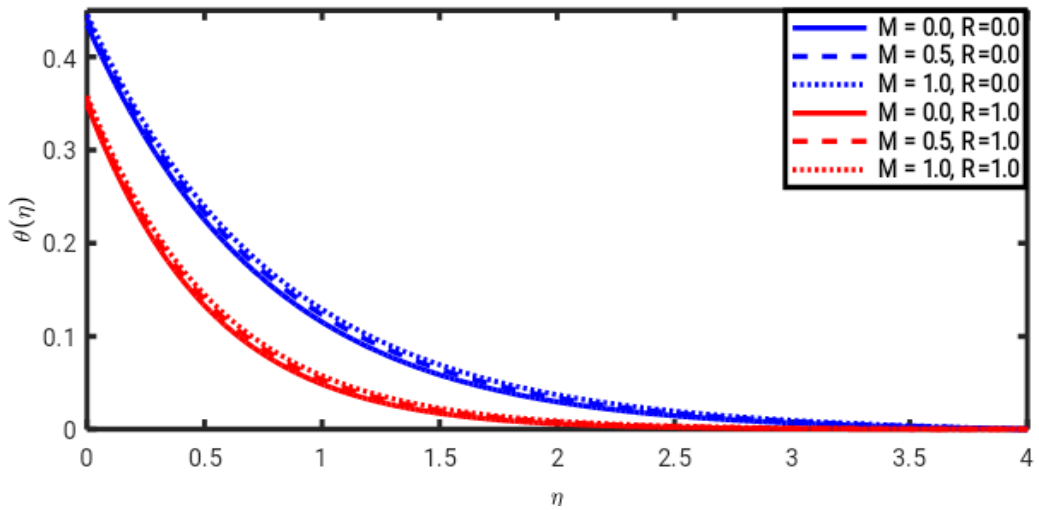

Fig.3 (b) Impact of M and R with no thermal slip on temperature $\Pr = 1, Sc = 10, f_w = 0.1, \lambda_1 = \lambda_2 = 0.2, S_f = 0.5, S_\theta = 1, S_\varphi = S_r = Kr = \eta = \delta = 0.5$

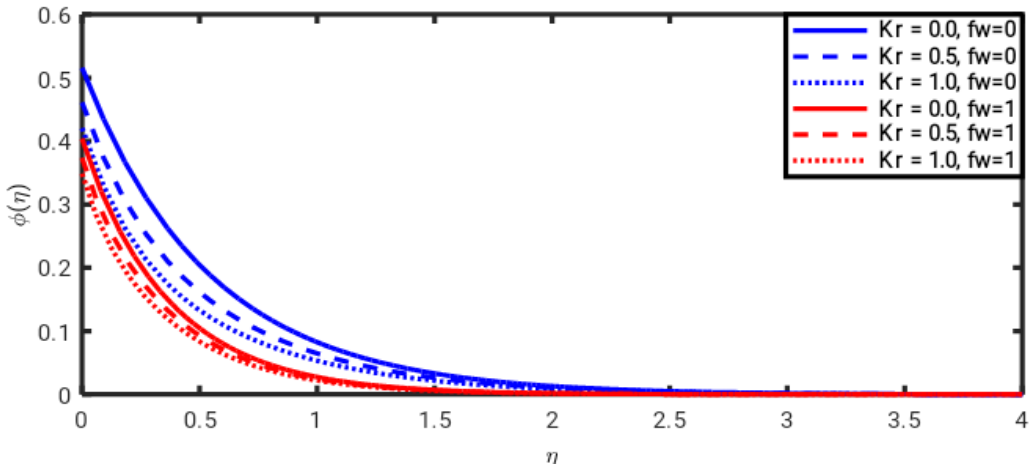

Fig.4 (a) Concentration impact of Kr and f_w on concentration without hydrodynamic slip $\Pr = 1, Sc = 10, \lambda_1 = \lambda_2 = 0.2, S_f = 0, S_\theta = S_\varphi = S_r = R = \eta = \delta = 0.5, M = 0.2$

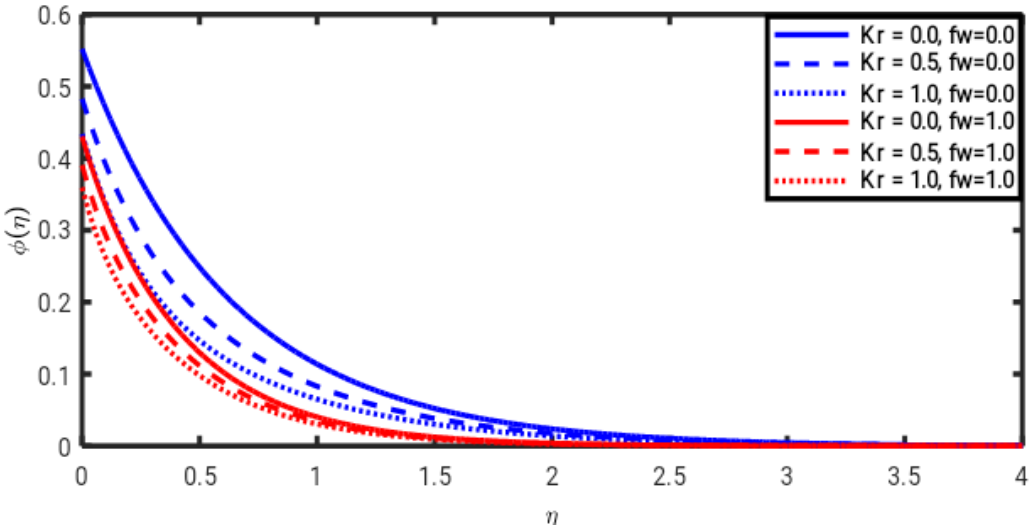

Fig.4(b) Concentration impact of Kr and f_w on concentration without hydrodynamic slip $\Pr = 1, Sc = 10, \lambda_1 = \lambda_2 = 0.2, S_f = 1, S_\theta = S_\varphi = S_r = R = \eta = \delta = 0.5, M = 0.2$

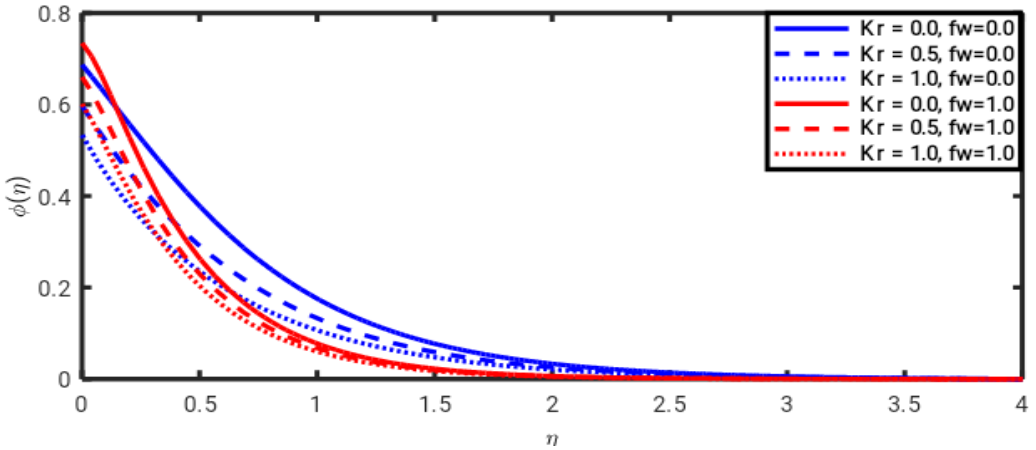

Fig.5(a) Concentration impact of Kr and f_w on concentration without thermal slip $\Pr = 1, Sc = 10, \lambda_1 = \lambda_2 = 0.2, S_f = 0.5, S_\theta = 0, S_\varphi = S_r = R = \eta = \delta = 0.5, M = 0.2$

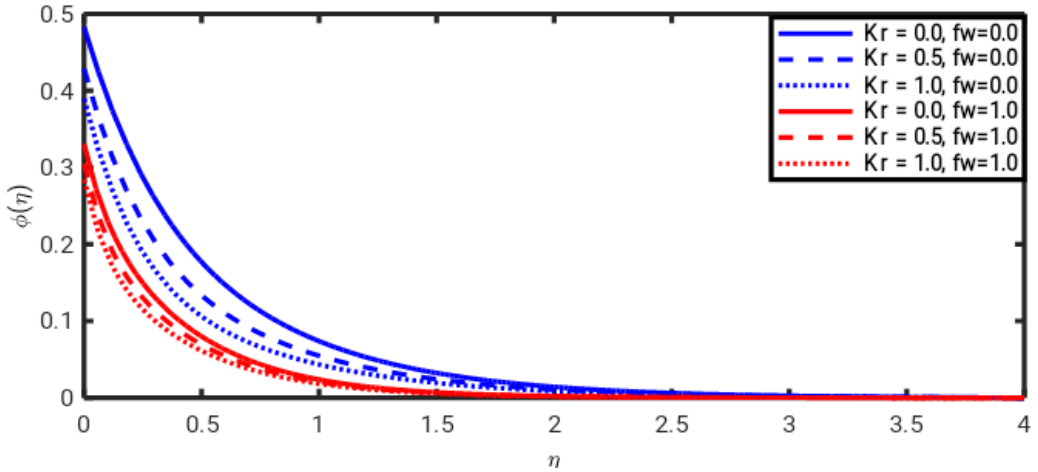

Fig.5(b) Concentration impact of Kr and f_w on concentration without thermal slip $\Pr = 1, Sc = 10, \lambda_1 = \lambda_2 = 0.2, S_f = 0.5, S_\theta = 1, S_\varphi = S_r = R = \eta = \delta = 0.5, M = 0.2$

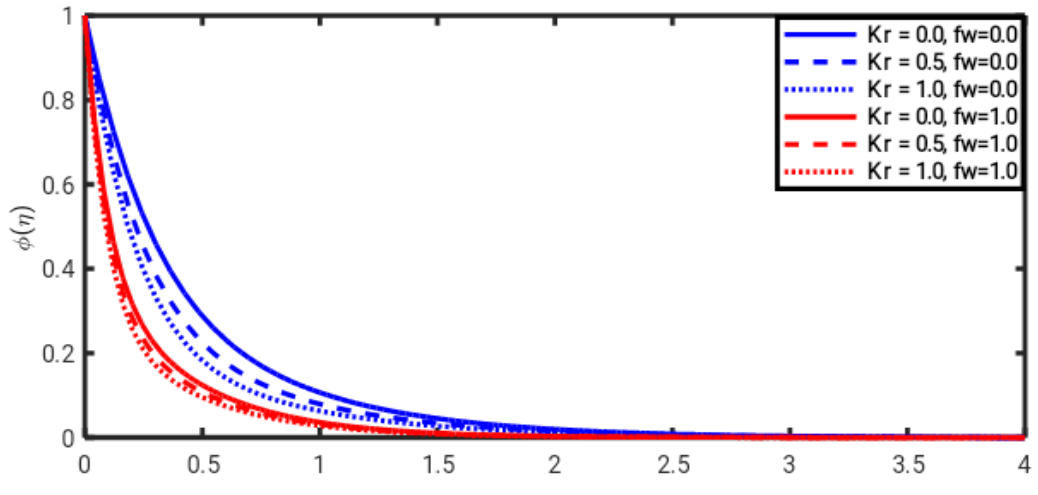

Fig.6(a) Concentration impact of Kr and f_w on concentration without solutal slip $\Pr = 1, Sc = 10, \lambda_1 = \lambda_2 = 0.2, S_f = S_\theta = 0.5, S_\varphi = 0, S_r = R = \eta = \delta = 0.5, M = 0.2$

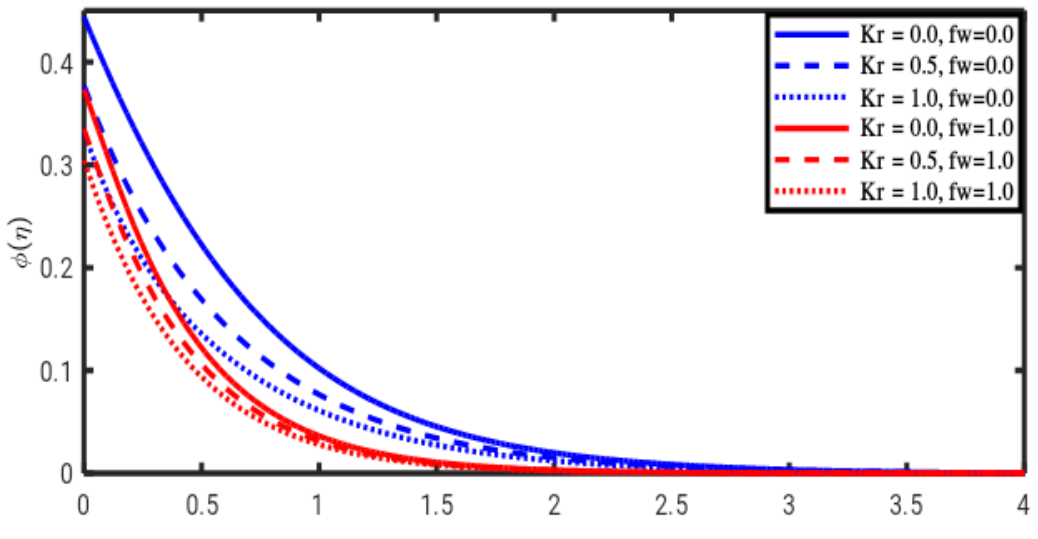

Fig.6(b) Concentration impact of Kr and f_w on concentration without solutal slip $\Pr = 1, Sc = 10, \lambda_1 = \lambda_2 = 0.2, S_f = S_\theta = 0.5, S_\varphi = 1, S_r = R = \eta = \delta = 0.5, M = 0.2$

Table 1: comparability of $-f''(0)$ for variant specifications of δ when $f_w = M = \lambda_1 = \lambda_2 = s_f = 0$

δ	Chamka et al. [2]	Maboodet al.[9]	Present study
0.8	1.261512	1.261042	1.265906
1.2	1.378052	1.377724	1.370847

Table.2 comparability of $-f''(0)$ for variant values of M when $f_w = \delta = s_f = 0$

M	Mabood and Das[7]	Maboodet al.[9]	Present study
1	1.4142135	1.41421356	1.414214
5	2.4494897	2.44948974	2.449490
10	3.3166247	3.31662479	3.316625
50	7.1414284	7.14142843	7.141428
100	10.049875	10.0498756	10.049875
500	22.383029	22.3830293	22.38029
1000	31.638584	31.6385840	31.638584

Table.3 comparability of heat transmission rate $-\theta'(0)$ for variant values of Pr when $M = f_w = S_f = S_\theta = \lambda_1 = \lambda_2 = R = 0$

Pr	Ali[1]	Maboodet al.[9]	Present study
0.72	0.8058	0.8088	0.809463
1.0	0.9691	1.0000	1.000063
3.0	1.9144	1.6237	1.923654
10	3.7006	3.7207	3.720649

Table.4 Variant in Mass transmission rate $-\varphi'(0)$ when $\Pr = M = f_w = S_f = S_\theta = S_\varphi = \lambda_1 = \lambda_2 = R = 0$

Kr	Sc	δ	$-\varphi'(0)$
0.0	1.0	0.5	**1.434017**
0.5	1.0	0.5	**1.610474**
1.0	1.0	0.5	**1.766765**
0.5	**0.0**	0.5	**0.250000**
0.5	**0.5**	0.5	**1.110829**
0.5	**1.0**	0.5	**1.610474**
0.5	1.0	**0.0**	**1.257990**
0.5	1.0	**0.5**	**1.610474**
0.5	1.0	**1.0**	**1.896832**

Our findings from the coefficient of skin friction produced by Chakma et al. [2] and Mabood and Standford[9] are compared in Table 1. There is a clear consensus with our results and these findings in this chart, i.e. the magnitude of skin friction rises with the stretching parameter values being increased.We notice a strong consensus in Table 2 between our current findings and the previous results obtained by Mabood and Das[7], Mabood and Standford[9]. Because of the growing Lorentz drag force induced by electromagnetism, it is understood that when the specification of magnetic objectM rises, skin friction enhances dramatically. The relation between our current findings and those obtained by Ali[1], Mabood, and Stanford[9] is seen in Table 3. We see that the Prandtl amount is much determined by the rate of heat transfer on the earth. The improvement in the number of Prandtl values contributes to an increase in the stretching board's heat transmission rate. The mass transmission rate for variant numbers of the chemical conversion specification, the Schmidt figure, and the unsteadiness parameter are shown in Table 4. It finds that the Schmidt number and unsteadiness parameter raises the rate of mass transmission as a chemical reaction parameter and, therefore, increase.

4.Conclusion

- Rising magnetic field values, suction, and slip parameters contribute to a diminishes in the stream's velocity.
- Rising thermal ration, magnetic object, and slip parameters result in fluid temperature change.

- The rise in the chemical conversionspecification, suction specification, and slip chemical reaction values contributes to a reduction in fluid concentration.

References

1. M.E.Ali (1994), Heat transfer characteristics of a continuous stretching surface, Warme- und Stoffubertragung, 29, 227-234.
2. A.J. Chamkha, A. M. Aly and M. A. Mansour (2010), Similarity Solution for Unsteady Heat and Mass Transfer from a Stretching Surface Embedded in a Porous Medium with Suction/Injection and Chemical Reaction Effects, Chemical Engineering Communications, 197, 846-858.
3. Swati Mukhopadhyay(2012), Slip effects on MHD boundary layer flow over an exponentially stretching sheet with suction/blowing and thermal radiation, Ain Shams Engineering Journal, 4, 485–491.
4. S. P. Anjali Devi1, D. Vasanthakumari(2014), Numerical investigation of slip flow effects on unsteady hydromagnetic flow over a stretching surface with thermal radiation, International journal of Advances in Applied Mathematics and Mechanics,1(4),20-32.
5. A.K. Abdul Hakeem, R. Kalaivananand N. Vishnu Ganesh, B. Ganga (2014), Effect of partial slip on hydromagnetic flow over a porous stretching sheet with non-uniform heat, source/sink, thermal radiation and wall mass transfer, Ain Shams Engineering Journal, 5, 913–922.
6. BadrAlkahtani, M. Subhas Abel,and Emad H. Aly(2015),Analysis of fluid motion and heat transport on magnetohydrodynamic boundary layer past a vertical power law stretching sheet with hydrodynamic and thermal slip effects,AIP Advances 5, 127228.
7. F. Mabood and K. Das(2016), Melting heat transfer on hydromagnetic flow of a nanofluid overa stretching sheet with radiation and second-order slip, The European Physical Journal Plus,131:3,1-12, DOI 10.1140/epjp/i2016-16003-1.
8. Shalini Jain and Amit Parmar(2018), Multiple Slip Effects on Inclined MHD Casson Fluid flow over a permeable stretching surface on a melting surface, International Journal of Heat and Technology, 36(2), 585-594.
9. FazleMabood and Stanford Shateyi(2019), Multiple Slip Effects on MHD Unsteady Flow Heat and Mass Transfer Impinging on Permeable Stretching Sheet with Radiation, Hindawi publishers, Modelling and Simulation in Engineering, Article ID 3052790, 1-11 .
10. Jawad Raja(2019), Thermal radiation and slip effects on magnetohydrodynamic (MHD) stagnation point flow of Casson fluid over a convective stretching sheet, Propulsion and Power Research,8(2), 138–146.
11. L.Th. Benos, U.S. Mahabaleshwar, P.H. Sakanakaand I.E. Sarris(2019), Thermal analysis of the unsteady sheet stretching subject to slip and magnetohydrodynamic effects, Thermal Science and Engineering and Progress, 13, 10367,1-8,
12. Faraz Faraz, Syed Muhammad Imran, Bagh Ali and Sajjad Haider(2019), Thermo-Diffusion and Multi-Slip Effect on an Axisymmetric Casson Flow over a UnsteadyRadially Stretching Sheet in the Presence of Chemical Reaction,Process(MDPI),7,1- 14, doi:10.3390/pr7110851.
13. U.S. Mahabaleshwara, K.R. Nagarajub, M.A. Sheremetc, D. Baleanud and E.Lorenzinie(2020), Mass transpiration on Newtonian flow over a porous stretching/shrinking sheet with slip, Chinese Journal of Physics, 63,130-137.
14. O.J. Fenuga(2020) , Mixed Convection In MHD Flow And Heat Transfer Rate Near A Stagnation-Point On A Non-Linear Vertical Stretching Sheet,International Journal of Applied Mechanics and Engineering, 25(1), 37-51,DOI: 10.2478/ijame-2020-0004.
15. SusheelaChaudharya, Santosh Chaudhary and Mohan Kumar Choudhary(2020), Numerical investigation of unsteady MHD flow and radiation heat transfer past a stretching surface in porous media with viscous dissipation and heat generation/absorption, Indian Journal of Pure & Applied Physics, 58, 71-78.